



**Supplementary Information for**

Early-life midazolam exposure persistently changes chromatin accessibility to impair adult hippocampal neurogenesis and cognition.

Correspondence to:

Taito Matsuda,

Department of Stem Cell Biology and Medicine,

Graduate School of Medical Sciences, Kyushu University,

3-1-1, Maidashi, Higashi-ku, Fukuoka 812-8582, Japan.

Phone: +81-92-642-6196; E-mail: [tmatsuda@scb.med.kyushu-u.ac.jp](mailto:tmatsuda@scb.med.kyushu-u.ac.jp)

Kinichi Nakashima,

Department of Stem Cell Biology and Medicine,

Graduate School of Medical Sciences, Kyushu University,

3-1-1, Maidashi, Higashi-ku, Fukuoka 812-8582, Japan.

Phone: +81-92-642-6195; E-mail: [kin1@scb.med.kyushu-u.ac.jp](mailto:kin1@scb.med.kyushu-u.ac.jp)

**This PDF file includes:**

Supplementary text

Figures S1 to S8

Tables S1 to S2

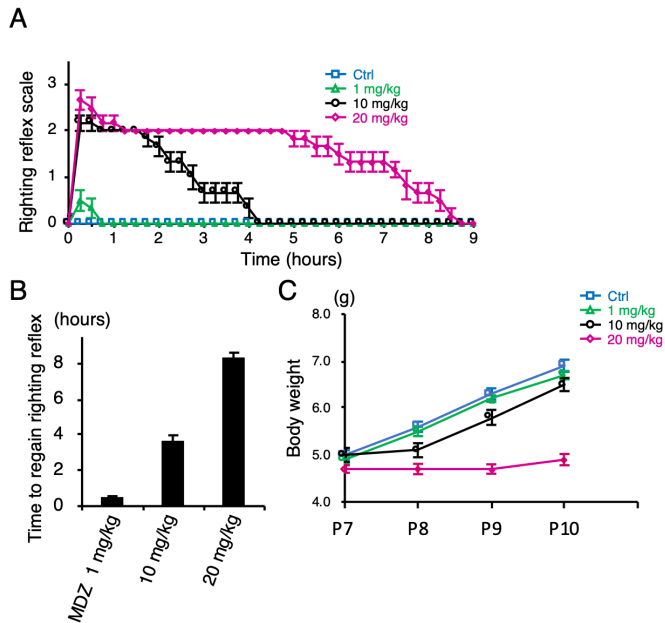


**Fig. S1: Sedation measurement after MDZ exposure.**

(A) Duration of sedation after MDZ treatment ( $n = 6$  animals each). (B) Bar graph showing time to recovery of righting reflex ( $n = 6$  animals each). MDZ treatment at 10 mg/kg is required for sedation without loss of body weight. (C) Body weight change after MDZ administration ( $n = 6$  animals each). MDZ treatment at 20 mg/kg abolishes body weight gain.

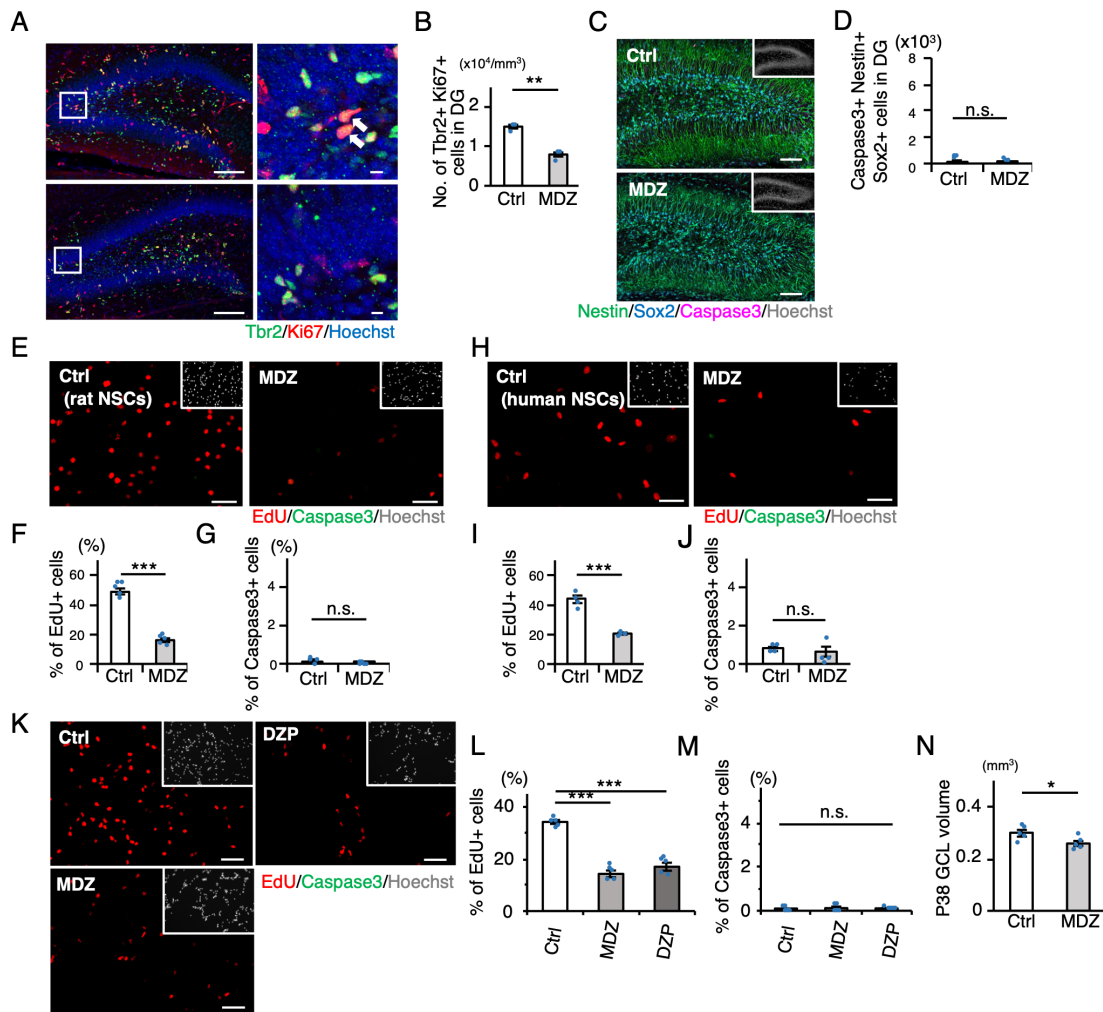


**Fig. S2: MDZ suppresses proliferation of rodent and human NSCs without inducing cell death.**

(A) Representative tile scan confocal images of immunostaining of Tbr2 (green), Ki67 (red), and Hoechst (blue) at P10. The areas outlined by a white rectangle are enlarged to the right. Arrows indicate Tbr2<sup>+</sup> Ki67<sup>+</sup> proliferating intermediate progenitor cells. Scale bars, 100  $\mu\text{m}$  (left) and 20  $\mu\text{m}$  (right). (B) Quantification of the number of Tbr2<sup>+</sup> Ki67<sup>+</sup> intermediate progenitor cells in the DG of Ctrl and MDZ mice at P10 ( $n = 3$  animals each).  $**P < 0.01$  by  $t$  test. (C) Representative tile scan confocal images of immunostaining of Nestin (green),

Sox2 (cyan), active Caspase 3 (magenta) and Hoechst (gray; insets). Scale bars, 100  $\mu\text{m}$ . (D) Quantification of the number of Caspase 3<sup>+</sup> Nestin<sup>+</sup> Sox2<sup>+</sup> NSCs in the DG of Ctrl and MDZ mice at P10 ( $n = 3$  animals each). (E) Representative images of EdU (red), active Caspase 3 (green) and Hoechst (gray; insets) staining in rat NSCs treated with MDZ (30  $\mu\text{M}$ ). Scale bars, 50  $\mu\text{m}$ . (F and G) Quantification of EdU<sup>+</sup> (F) or Caspase 3<sup>+</sup> (G) cells in (E) ( $n = 5$  animals each). (H) Representative images of EdU (red), active Caspase 3 (green) and Hoechst (gray; insets) staining in human NSCs treated with MDZ (30  $\mu\text{M}$ ). Scale bars, 50  $\mu\text{m}$ . (I and J) Quantification of EdU<sup>+</sup> (I) or Caspase 3<sup>+</sup> (J) cells in (H) ( $n = 4$  animals each). (K) Representative images of EdU (red), active Caspase 3 (green) and Hoechst (gray; insets) staining in mouse NSCs treated with MDZ (30  $\mu\text{M}$ ) or diazepam (DZP, 50  $\mu\text{M}$ ) for 24 hours. (L and M) Quantification of EdU<sup>+</sup> (L) or Caspase 3<sup>+</sup> (M) cells in (K) ( $n = 5$  animals each). (N) Quantification of volume of GCL ( $\text{mm}^3$ ) of Ctrl and MDZ mice at P38 ( $n = 6$  animals per group). \*\*\* $P < 0.001$  by ANOVA with Tukey post-hoc tests (L and M) and \* $P < 0.05$  and \* $P < 0.01$  by  $t$  test (B, F, I and N). n.s., not significant.

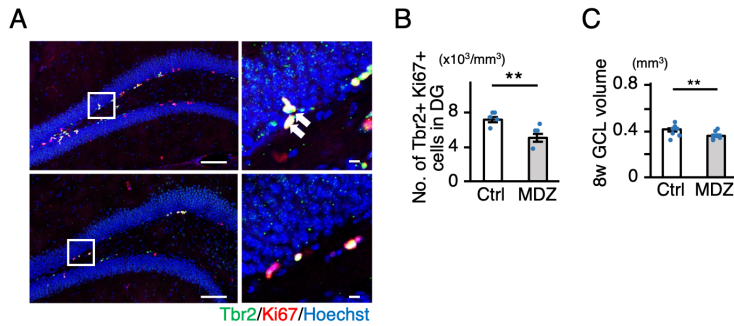


**Fig. S3: MDZ suppresses proliferation of progenitor cells in the adult DG.**

(A) Representative tile scan confocal images of immunostaining of Tbr2 (green), Ki67 (red), and Hoechst (blue) at 8w. The areas outlined by a white rectangle are enlarged to the right. Arrows indicate Tbr2<sup>+</sup> Ki67<sup>+</sup> proliferating intermediate progenitor cells. Scale bars, 100  $\mu$ m (left) and 20  $\mu$ m (right). (B) Quantification of the number of Tbr2<sup>+</sup> Ki67<sup>+</sup> intermediate progenitor cells in the DG of Ctrl and MDZ mice at 8w ( $n = 3$  animals each).  $**P < 0.01$  by  $t$  test. (C) Quantification of volume of GCL (mm<sup>3</sup>) of Ctrl and MDZ mice at 8w ( $n = 6$  animals per group).  $*P < 0.01$  by  $t$  test.

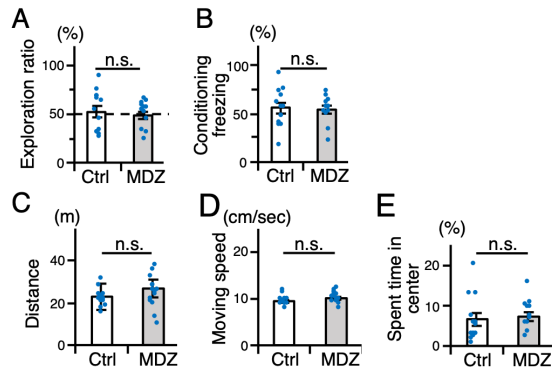


**Fig. S4: Behavioral analysis of MDZ-exposed mice.**

(A) Exploration ratio in Ctrl ( $n = 12$ ) and MDZ ( $n = 12$ ) mice during familiarization. Ctrl and MDZ-treated mice showed comparable levels of exploration of the test object. (B) Ctrl ( $n = 13$ ) and MDZ ( $n = 14$ ) mice showed an equivalent freezing response in the conditioning phase before the testing phase. (C–E) Bar graphs showing the distance traveled throughout the open field (C), moving speed (D), and the percentage of time spent in the center (E). MDZ treated mice exhibited no difference in locomotive activity or anxiety level compared to Ctrl mice. n.s., not significant.

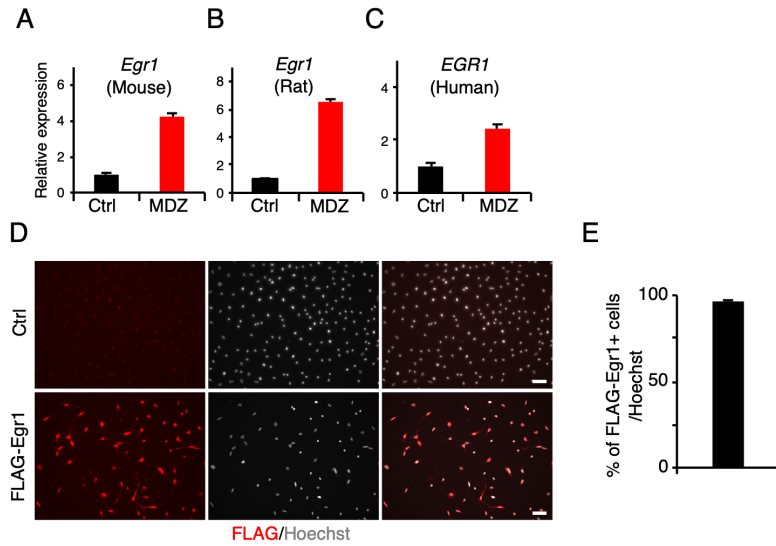


**Fig. S5: Egr1 expression in cultured mouse NSCs.**

(A–C) Relative expression of *Egr1* after MDZ treatment (30  $\mu$ M) in cultured mouse (A), rat (B), and human (C) NSCs. (D) Representative images of FLAG-tagged Egr1 (red) and Hoechst at 24 h after the induction of Egr1 expression in cultured mouse NSCs. (E) Bar graph showing the percentage of FLAG-tagged Egr1<sup>+</sup> cells among Hoechst<sup>+</sup> cells.

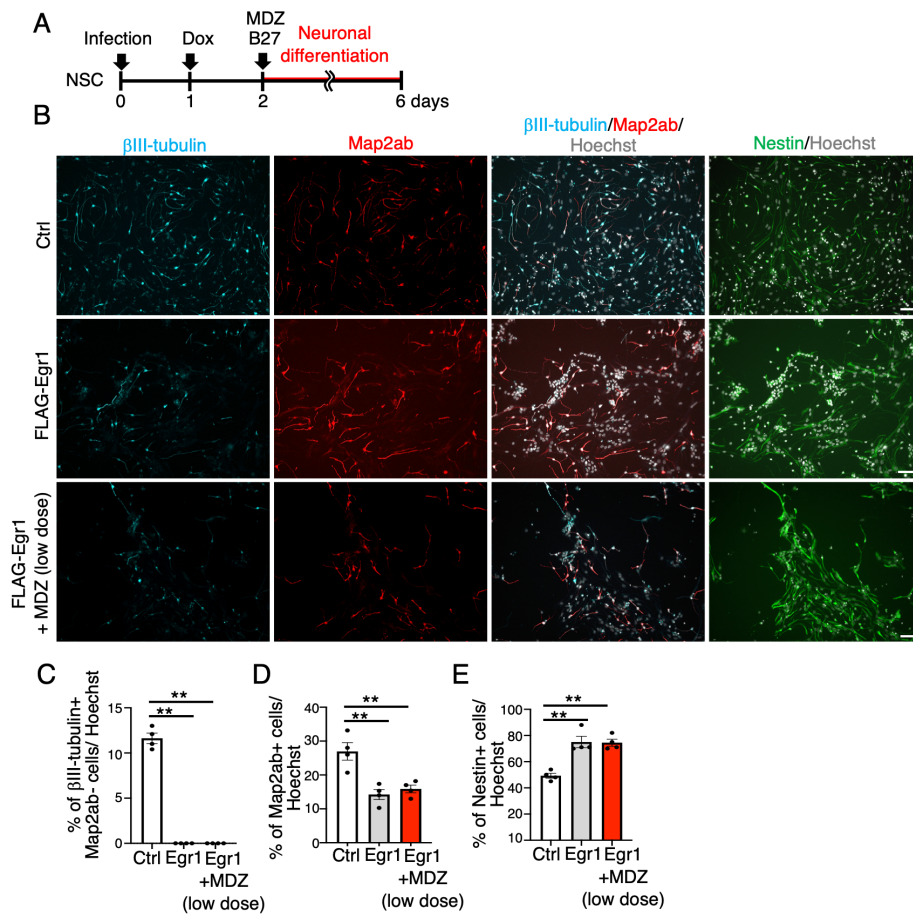


**Fig. S6: Egr1 represses neuronal differentiation of NSCs.**

(A) Experimental scheme for investigating the neuronal differentiation of Egr1-transduced NSCs. (B) Representative images of immunostaining of  $\beta$ III-tubulin (cyan), Map2ab (red), Nestin (green), and Hoechst (gray) at 5 d after doxycycline-induced Egr1 expression. (C and D) Quantification of  $\beta$ III-tubulin<sup>+</sup> (C), Map2ab<sup>+</sup> (D) and Nestin<sup>+</sup> (E) cells in (B) (n = 4). \*\*P < 0.01 by ANOVA with Tukey post-hoc tests.



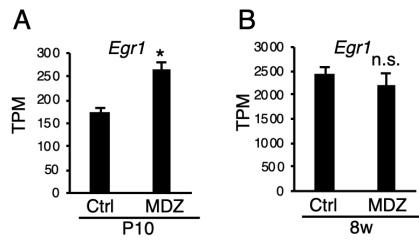


**Fig. S7: Transient up-regulation of *Egr1* after MDZ exposure.**

(A and B) Bar graphs showing the expression levels of *Egr1* in Nestin-GFP<sup>+</sup> cells in the DG at P10 (A) and 8w (B) ( $n = 3$ ). \* $q < 0.05$ . n.s., not significant.

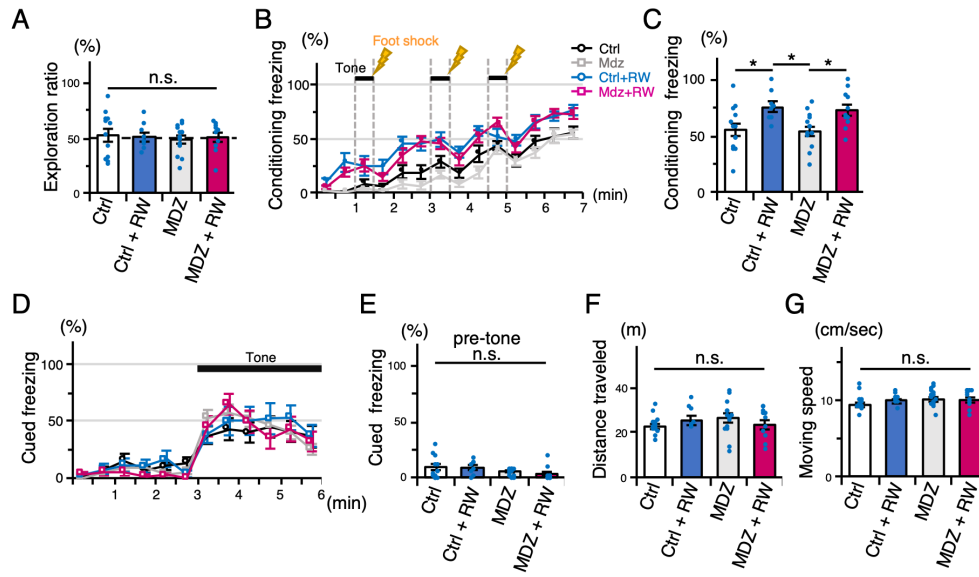


**Fig. S8: Behavioral analysis of MDZ-exposed mice after voluntary running.**

(A) Exploration time in each group during the familiarization phase. All 4 groups showed comparable levels of exploration of the test object (Ctrl ( $n = 13$ ), Ctrl+RW ( $n = 8$ ), MDZ ( $n = 14$ ), and MDZ+RW ( $n = 11$ ) mice). (B and C) Time course of freezing response (B) and quantification of freezing rate (C) in the conditioning phase.  $*P < 0.05$  by ANOVA with Tukey post-hoc tests. (D and E) Time course of freezing response (D) and quantification of freezing rate (E) prior to the tone in the cued FC test (Ctrl ( $n = 13$ ), Ctrl+RW ( $n = 8$ ), MDZ ( $n = 14$ ), and MDZ+RW ( $n = 11$ ) mice). (F and G) Bar graphs showing the distance traveled throughout the open field (F) and the moving speed (G) (Ctrl ( $n = 13$ ), Ctrl+RW ( $n = 8$ ), MDZ ( $n = 14$ ), and MDZ+RW ( $n = 11$ ) mice). Mice with or without running exhibited no difference in locomotive activity. n.s., not significant.

**Table S1: List of quiescence-associated factors**

| No. | Gene Name     | Reference  |
|-----|---------------|--|
| 1   | <b>Pten</b>   | M. Groszer, et al., PTEN negatively regulates neural stem cell self-renewal by modulating G0-G1 cell cycle entry. <i>Proc Natl Acad Sci U S A.</i> 103, 111–116 (2006).  |
| 2   | <b>Id1</b>    | H. Nam, et al., High levels of Id1 expression define B1 type adult neural stem cells. <i>Cell Stem Cell.</i> 5, 515–526 (2009).  |
| 3   | <b>Foxo3</b>  | J. Paik, et al., FoxOs Cooperatively Regulate Diverse Pathways Governing Neural Stem Cell Homeostasis. <i>Cell Stem Cell.</i> 5, 540–553 (2009). ; V. M. Renault, et al., FoxO3 regulates neural stem cell homeostasis. <i>Cell Stem Cell.</i> 5, 527–539 (2009).  |
| 4   | <b>Smad4</b>  | H. Mira, et al., Signaling through BMPR-1A regulates quiescence and long-term activity of neural stem cells in the adult hippocampus. <i>Cell Stem Cell.</i> 7, 78–89 (2010).  |
| 5   | <b>Bmpr1a</b> | H. Mira, et al., Signaling through BMPR-1A regulates quiescence and long-term activity of neural stem cells in the adult hippocampus. <i>Cell Stem Cell.</i> 7, 78–89 (2010).  |
| 6   | <b>Rest</b>   | Z. Gao, et al., The master negative regulator REST/NRSF controls adult neurogenesis by restraining the neurogenic program in quiescent stem cells. <i>J Neurosci.</i> 31, 9772–9786 (2011).  |
| 7   | <b>Vcam1</b>  | E. Kokovay, et al., VCAM1 is essential to maintain the structure of the SVZ niche and acts as an environmental sensor to regulate SVZ lineage progression. <i>Cell Stem Cell.</i> 11, 220–230 (2012).  |
| 8   | <b>Nfix</b>   | B. Martynoga, et al., Epigenomic enhancer annotation reveals a key role for NFIX in neural stem cell quiescence. <i>Genes Dev.</i> 27, 1769–1786 (2013).   |
| 9   | <b>Cdkn1a</b> | E. Porlan, et al., Transcriptional repression of Bmp2 by p21Waf1/Cip1 links quiescence to neural stem cell maintenance. <i>Nat Neurosci.</i> 16, 1567–1575 (2013).   |
| 10  | <b>Cdkn1c</b> | S. Furutachi, et al., P57 controls adult neural stem cell quiescence and modulates the pace of lifelong neurogenesis. <i>EMBO J.</i> 32, 970–981 (2013).   |
| 11  | <b>Dll1</b>   | D. Kawaguchi, et al., Dll1 maintains quiescence of adult neural stem cells and segregates asymmetrically during mitosis. <i>Nat Commun.</i> 4, 1–12 (2013).  |
| 12  | <b>Cdh2</b>   | E. Porlan, et al., MT5-MMP regulates adult neural stem cell functional quiescence through the cleavage of N-cadherin. <i>Nat Cell Biol.</i> 16, 629–638 (2014).  |
| 13  | <b>Gabbr1</b> | C. Giachino, et al., GABA suppresses neurogenesis in the adult hippocampus through GABAB receptors. <i>Development.</i> 141, 83–90 (2014).   |
| 14  | <b>Hopx</b>   | D. Li, et al., Hopx distinguishes hippocampal from lateral ventricle neural stem cells. <i>Stem Cell Res.</i> 15, 522–529 (2015).  |
| 15  | <b>Sox2</b>   | A. Amador-Arjona, et al., SOX2 primes the epigenetic landscape in neural precursors enabling proper gene activation during hippocampal neurogenesis. <i>Proc Natl Acad Sci U S A.</i> 112, E1936–E1945 (2015).   |
| 16  | <b>Pros1</b>  | K. Zelensova, et al., Protein S regulates neural stem cell quiescence and neurogenesis. <i>Stem Cells.</i> 35, 679–693 (2017).   |
| 17  | <b>Mfge8</b>  | Y. Zhou, et al., Autocrine Mfge8 Signaling prevents developmental exhaustion of the adult neural stem cell pool. <i>Cell Stem Cell.</i> 23, 444–452.e4 (2018).   |
| 18  | <b>Id4</b>    | R. Zhang, M. et al., Id4 downstream of Notch2 maintains neural stem cell quiescence in the adult hippocampus. <i>Cell Rep.</i> 28, 1485–1498.e6 (2019).  |
| 19  | <b>Notch2</b> | Same as above  |
| 20  | <b>Hes5</b>   | Same as above  |
| 21  | <b>Hes1</b>   | I. Luque-Molina, et al., The orphan nuclear receptor TLX represses Hes1 expression, thereby affecting NOTCH signaling and lineage progression in the adult SEZ. <i>Stem Cell Reports.</i> 13, 132–146 (2019).; R. Stueda, et al., High Hes1 expression and resultant Ascl1 suppression regulate quiescent vs. active neural stem cells in the adult mouse brain. <i>Genes Dev.</i> 33, 511–523 (2019). |
| 22  | <b>Egr1</b>   | This study   |

**Table S2: Top 10 up-regulated and down-regulated genes at P10.**

| Up            |             |             | References associated with stem cell quiescence  |
|---------------|-------------|-------------|--|
| Gene          | Fold change | q-value     |  |
| Nab2          | 0.559971366 | 3.07E-07    | -  |
| Gm12504       | 0.54608964  | 1.20E-08    | -  |
| Meox1         | 0.517183233 | 0.000362172 | -  |
| Egr3          | 0.503974661 | 0.000499342 | -  |
| Frs3          | 0.491933285 | 3.42E-05    | -  |
| Jade2         | 0.49117208  | 0.000499342 | -  |
| A330093E20Rik | 0.483481999 | 0.000279103 | -  |
| Egr1          | 0.482020383 | 6.39E-06    | L. M. Min, et al., The transcription factor EGR1 controls both the proliferation and localization of hematopoietic stem cells. <i>Cell Stem Cell</i> , <b>2</b> , 380–391 (2008).      |
| Ier2          | 0.479184607 | 5.60E-05    | -  |
| Nr4a1         | 0.476795492 | 7.73E-05    | P. R. Freire, et al., NR4A1 and NR4A3 restrict HSC proliferation via reciprocal regulation of C/EBP $\alpha$ and inflammatory signaling. <i>Blood</i> , <b>131</b> , 1081–1093 (2018). |

| Down    |             |             | References associated with stem cell quiescence |
|---------|-------------|-------------|---|
| Gene    | Fold change | q-value     |   |
| Fmod    | -0.55241454 | 3.09E-05    | -   |
| Cfh     | -0.5250434  | 0.000217271 | -   |
| Lamc3   | -0.50422156 | 0.000377014 | -   |
| Coll8a1 | -0.46869736 | 0.000177616 | -   |
| Colec12 | -0.45339981 | 0.000780575 | -   |
| Ctsk    | -0.43126638 | 0.006331009 | -   |
| Filip11 | -0.42877304 | 0.004962135 | -   |
| Aoc3    | -0.42165482 | 0.008230287 | -   |
| Rnase1  | -0.41906401 | 0.000420459 | -   |
| Ii33    | -0.41758698 | 0.003325697 | -   |